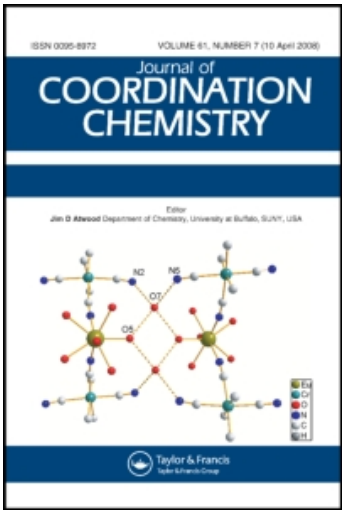

Journal of Coordination Chemistry
Publication details, including instructions for authors and subscription information:
http://www.informaworld.com/smpp/title~content=t713455674

The first ruthenium(II) complex with benzotriazole and pyridylcarboxylato ligands

J. G. Małecki[a]; J. Kusz[b]
[a] Department of Inorganic and Radiation Chemistry, Institute of Chemistry, University of Silesia, Katowice, Poland [b] Institute of Physics, University of Silesia, Katowice

To cite this Article Małecki, J. G. and Kusz, J.(2007) 'The first ruthenium(II) complex with benzotriazole and pyridylcarboxylato ligands', Journal of Coordination Chemistry, 60: 22, 2461 — 2470
To link to this Article: DOI: 10.1080/00958970701275022
URL: http://dx.doi.org/10.1080/00958970701275022

Journal of Coordination Chemistry
Vol. 60, No. 22, 15 November 2007, 2461–2470

Taylor & Francis
Taylor & Francis Group

The first ruthenium(II) complex with benzotriazole and pyridylcarboxylato ligands

J. G. MAŁECKI*† and J. KUSZ‡

†Department of Inorganic and Radiation Chemistry, Institute of Chemistry, University of Silesia, 9th Szkolna St., 40-006, Katowice, Poland
‡Institute of Physics, University of Silesia, 4th Uniwersytecka St., 40-006, Katowice

(*Received 2 December 2006; revised 7 December 2006; in final form 11 December 2006*)

The reaction of $[RuCl_2(PPh_3)_3]$ with 1-(2-pyridylcarbonyl)benzotriazole has been examined. A new ruthenium(II) complex – $[RuCl(PPh_3)_2(C_6H_5N_3)(C_5H_4NCO_2)]$ has been obtained and characterized by IR and UV–Vis measurements. The crystal structure of the complex has been determined. The electronic spectrum of the complex has been calculated by TDDFT method.

Keywords: Ruthenium; Benzotriazole; Phosphine; X-ray structure; TDDFT method

1. Introduction

Metal complexes of aldehydes and ketones have been considered as possible models for catalytic intermediates in the transfer hydrogenation of ketones by alcohols. Many ruthenium(II)-based catalysts for transfer hydrogenation are known, but the intermediates in the catalytic process remain a matter of debate. Several mechanistic proposals suggest that the key step involves activation of the coordinated substrate, making ruthenium(II) ketone and aldehyde complexes of interest [1]. Transition metal complexes containing nitrogen and oxygen donor ligands have been of interest for many years due to their steric and electronic properties [2–6].

The five-coordinate ruthenium(II) complex $[RuCl_2(PPh_3)_3]$ is well known as a very useful precursor for the preparation of a wide range of ruthenium compounds, including N-donor derivatives [7–10].

Density functional theory (DFT) is a very popular computational method for calculation of a number of molecular properties. Because of its computational efficiency, DFT has been applied extensively to inorganic and organometallic complexes [11–15]. Time-dependent generalization of DFT (TDDFT) offers a rigorous route to calculate the dynamic response of charge density [16–18]. The reliability of TDDFT in obtaining accurate predictions of excitation energies and oscillator strengths is well documented, used to calculate the electronic spectra of transition metal

*Corresponding author. Email: gmalecki@us.edu.pl

Journal of Coordination Chemistry
ISSN 0095-8972 print/ISSN 1029-0389 online © 2007 Taylor & Francis
DOI: 10.1080/00958970701275022

complexes with a variety of ligands [19–21]. TDDFT gives fairly accurate results for valence excited states but incorrectly describes long-range excited states of CT character. This failure was ascribed to the self-interaction error in DFT or alternatively to incorrect asymptotic behaviour of the approximate density functional [22]. The influence HF exchange in hybrid functional on the calculated energies of CT states was studied for ruthenium complexes [23].

In this article we present the synthesis, spectroscopic properties and molecular structure of ruthenium(II) complex with benzotriazole and pyridylcarboxylato ligands, prepared in the reaction between $[RuCl_2(PPh_3)_3]$ and 1-(2-pyridylcarbonyl)benzotriazole in methanolic solution. The ligand hydrolyses to give the benzotriazole and pyridylcarboxylate ligands, catalyzed by the ruthenium complex. Ruthenium compounds are known catalysts in hydrolysis [24].

Attempted synthesis of the same complex using an equimolar mixture of benzotriazole and 2-pyridylcarboxylate failed.

2. Experimental

All reagents used in synthesis of the complex are commercially available and were used without further purification. The $[RuCl_2(PPh_3)_3]$ complex was synthesized according to the literature method [25].

The complex was prepared by adding 2-(2-pyridylcarbonyl)benzotriazole (0.1 g, 4.5×10^{-4} mol) to a solution of $[RuCl_2(PPh_3)_3]$ (0.2 g, 2.1×10^{-4} mol) in methanol (100 mL). The reaction mixture was stirred overnight. The obtained solution was filtered and crystals of $[RuCl(PPh_3)_2(C_6H_5N_3)(C_5H_4NCO_2)]$ suitable for X-ray analysis were obtained by slow evaporation of a methanolic solution. Yield 75%. Anal. Calcd for $C_{48}H_{38}N_4O_2P_2ClRu$: C 63.89%; H 4.36%; N 6.21%. Found: C 63.95%; H 4.27%; N 6.24%. IR (KBr): 3057 (ν_{CH}); 1963 (ν_{Ph}); 1896 (ν_{Ph}); 1622 ($\nu_{C=N}$), 1591 (ν_{asCOO}); 1482 (ν_{ring}); 1435 ($\nu_{C=C}$); 1385 (ν_{sCOO}); 1175 (δ_{CH}); 1119 (ν_{C-COO}); 1091 (δ_{CH}); 694 (δ_{ring}). UV–Vis (CH_2Cl_2): 381.6 (3.63) 259.0 (4.33), 233.2 (4.64), 217.2 (4.45).

2.1. *Physical measurements*

Infrared spectra were recorded on a Nicolet Magna 560 spectrophotometer in the spectral range 4000–400 cm^{-1} with KBr pellets. The electronic spectrum was measured on a spectrophotometer Lab Alliance UV–Vis 8500 in the range 600–180 nm in dichloromethane. Elemental analyses (C, H, N) were performed on a Perkin–Elmer CHN-2400 analyzer.

2.2. *Crystal structure determination and refinement*

X-ray intensity data were collected with graphite monochromated Mo-Kα radiation ($\lambda = 0.71073$ Å) at room temperature on a Kuma Diffraction KM4 diffractometer and processed with the Omnibus-BLP data processing program [26]. Details concerning crystal data and refinement are given in table 1. Lorentz polarization and empirical absorption corrections were applied. The structures were solved by Patterson and Fourier methods. All non-hydrogen atoms were refined anisotropically using full-matrix, least-squares techniques. The hydrogen atoms of the phenyl rings were treated

Table 1. Crystal data and structure refinement details of $[RuCl(PPh_3)_2(C_6H_5N_3)(C_5H_4NCO_2)]$.

Empirical formula	$C_{48}H_{38}ClN_4O_2P_2Ru$
Formula weight	901.28
Temperature (K)	293(2)
Crystal system	Triclinic
Space group	$P\bar{1}$
Unit cell dimensions (Å, °)	
a	12.194(2)
b	12.384(3)
c	15.160(3)
α	78.46(3)
β	74.74(3)
γ	81.33(3)
Volume (Å^3)	2152.2(7)
Z	2
Calculated density (Mg m^{-3})	1.391
Absorption coefficient (mm^{-1})	0.544
$F(000)$	922
Crystal dimensions (mm^3)	$0.08 \times 0.10 \times 0.30$
Range for data collection (°)	2.83–32.87
Index ranges	$-17 \le h \le 18$, $-18 \le k \le 18$, $-16 \le l \le 22$
Reflections collected	20872
Independent reflections	13277 [R(int) = 0.0392]
Data/restraints/parameters	13277/0/523
Goodness-of-fit on F^2	0.651
Final R indices [$I > 2\sigma(I)$]	$R_1 = 0.0369$, $wR_2 = 0.0500$
R indices (all data)	$R_1 = 0.1390$, $wR_2 = 0.0573$
Largest diff. Peak and hole (e Å^{-3})	0.456 and −0.295

as 'riding' on their parent carbon atoms [d(C–H) = 0.96 Å] and assigned isotropic temperature factors 1.2 times the value of equivalent temperature factor of the parent carbon atom. SHELXS97 [27], SHELXL97 [28] and SHELXTL [29] programmes were used for all the calculations.

2.3. *Computational details*

Gaussian 03 [30] was used in the calculations. The geometry optimisation was carried out with the DFT method with the use of B3LYP functional [31, 32]. The electronic spectrum of the complex was calculated with the PCM model [33] in dichloromethane solution. The DZVP basis set [34] with F functions with exponents 1.94722036 and 0.748930908 on ruthenium and polarization and diffuse functions to all other atoms (6-31+g**) were used.

3. Results and discussion

Reaction between 1-(2-pyridylcarbonyl)benzotriazole and $[RuCl_2(PPh_3)_3]$ in methanolic solution gave $[RuCl(PPh_3)_2(C_6H_5N_3)(C_5H_4NCO_2)]$ with good yields. The elemental analysis of the complex is in good agreement with its formulation.

Infrared spectrum of the complex exhibits the characteristic bands of the COO stretching mode, asymmetric at 1591 cm^{-1} and symmetric at 1385 cm^{-1}. The C=N stretching modes are at 1622 cm^{-1}. The $\nu_{Ph(P-Ph)}$ absorption band is at 1435 cm^{-1} and bands characteristic to phenyl vibrations are at 1963 and 1896 cm^{-1}.

The complex crystallizes in the triclinic $P\bar{1}$ space group. The molecular structure of the compound is shown in figure 1 (structural drawing of the complex is presented in figure 2) and selected bond lengths and angles are listed in table 2.

The ruthenium is distorted octahedral geometry with *cis* phosphine ligands and *cis* benzotriazole and 2-pyridylcarboxylate (see table 2). All Ru-ligand distances, such as Ru–Cl 2.4095(10) Å, Ru–P 2.3368(9) and 2.3383(8) Å, and Ru–N 2.1217(18) and 2.1451(19) Å and Ru–O 2.0965(15) Å, are normal and comparable with distances in other ruthenium complexes containing the heterocyclic ligands [35–37].

The conformation of the molecule is stabilized by four C–H···Cl weak intramolecular hydrogen bonds [38–40] (D···A distance varies from 3.49(8) to 3.31(9) Å and D–H···A angle varies from 154.0 to 120.0°) and two C–H···O hydrogen bonds linking C(16)–H(63)···O(5) (D···A distance 3.092(10) Å, D–H···A angle 142.0°) and C(40)–H(83)···O(5) (D···A distance 3.13(9) Å, D–H···A angle 149.0°) (see table 3).

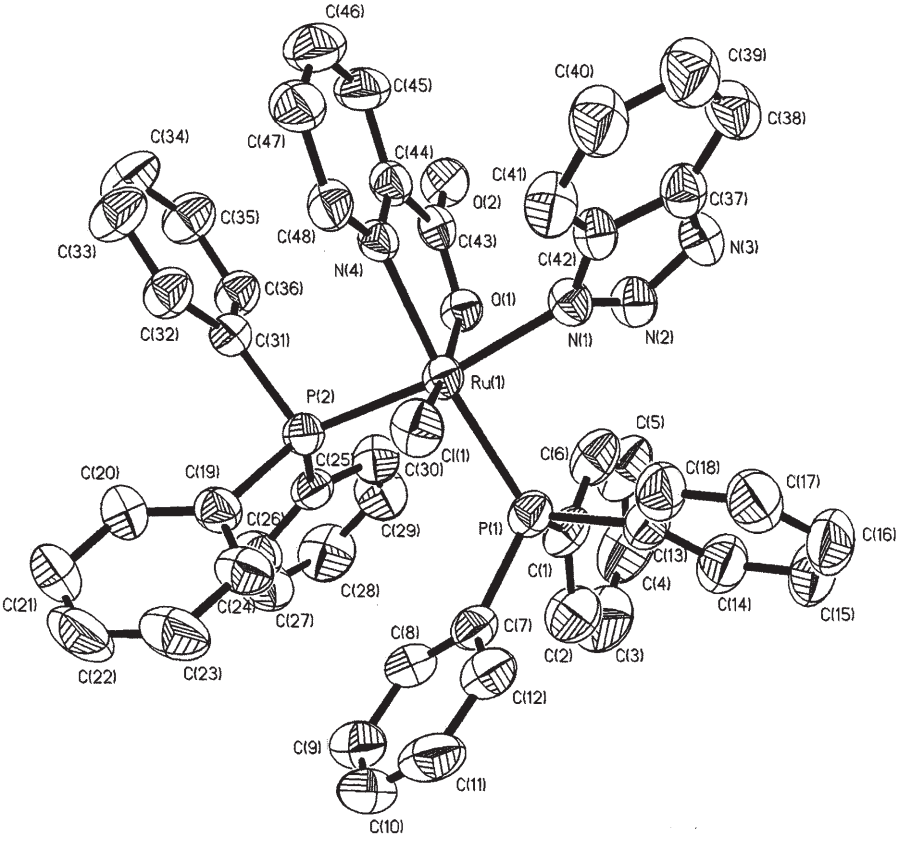

Figure 1. ORTEP drawing of $[RuCl(PPh_3)_2(C_6H_5N_3)(C_5H_4NCO_2)]$ with 50% probability thermal ellipsoids.

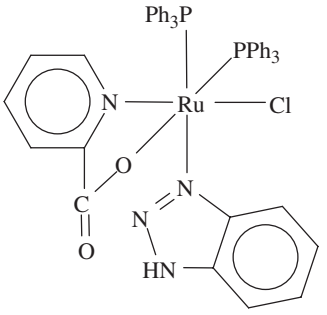

Figure 2. Structural drawing of $[RuCl(PPh_3)_2(C_6H_5N_3)(C_5H_4NCO_2)]$.

Table 2. Selected bond lengths (Å) and angles (°) for $[RuCl(PPh_3)_2(C_6H_5N_3)(C_5H_4NCO_2)]$.

	Experimental	Calculated
Ru(1)–O(1)	2.0965(15)	2.119
Ru(1)–N(4)	2.1217(18)	2.149
Ru(1)–N(1)	2.1451(19)	2.201
Ru(1)–P(1)	2.3368(9)	2.426
Ru(1)–P(2)	2.3383(8)	2.435
Ru(1)–Cl(1)	2.4095(10)	2.501
O(1)–Ru(1)–N(4)	77.81(7)	77.58
O(1)–Ru(1)–N(1)	83.40(7)	84.94
N(4)–Ru(1)–N(1)	82.98(7)	82.72
O(1)–Ru(1)–P(1)	99.44(5)	98.45
N(4)–Ru(1)–P(1)	172.45(5)	170.72
N(1)–Ru(1)–P(1)	89.74(6)	87.26
O(1)–Ru(1)–P(2)	88.33(5)	87.13
N(4)–Ru(1)–P(2)	90.18(6)	87.26
N(1)–Ru(1)–P(2)	170.21(5)	169.49
P(1)–Ru(1)–P(2)	96.79(4)	98.69
O(1)–Ru(1)–Cl(1)	168.10(4)	169.33
N(4)–Ru(1)–Cl(1)	91.31(6)	92.64
N(1)–Ru(1)–Cl(1)	90.56(6)	91.81
P(1)–Ru(1)–Cl(1)	90.75(4)	91.80
P(2)–Ru(1)–Cl(1)	96.61(3)	94.27

3.1. *Geometry and electronic structure*

The optimized geometry parameters for the studied complex are given in table 2. The calculated bond lengths and angles for $[RuCl(PPh_3)_2(C_6H_5N_3)(C_5H_4NCO_2)]$ agree with the experiment, the largest differences are found for the ruthenium–chlorine and Ru–P bonds (~0.09 Å). The maximum differences between the calculated and experimental angles is for N(4)–Ru(1)–P(2) at 2.9°.

The formal charge of ruthenium is +2 in this complex. The calculated charge on ruthenium, obtained from natural population analysis, is close 0.4015. The population of the d_{xy}, d_{xz}, d_{yz}, $d_{x^2-y^2}$ and d_z^2 orbitals of Ru^{2+} is 1.7997, 1.9028, 1.883, 0.9442 and 0.7851, respectively. This is a result of charge donation from chlorine (charge −0.6197) and phosphine molecules to ruthenium atom. The charges obtained from NBO analysis on the benzotriazole and 2-pyridylcarboxylato ligands are 0.142 and −0.555, respectively. The HOMO–LUMO gap is 3.18 eV.

Table 3. Hydrogen bonds for $[RuCl(PPh_3)_2(C_6H_5N_3)(C_5H_4NCO_2)]$ (Å and °).

D–H···A	d(D–H)	d(H···A)	d(D···A)	∠(DHA)
C(16)–H(63)···O(5)	1.08	2.16	3.092(10)	142.0
C(28)–H(73)···Cl(2)	1.09	2.48	3.49(8)	154.0
C(34)–H(78)···Cl(2)	1.08	2.63	3.31(9)	120.0
C(40)–H(83)···O(5)	1.08	2.15	3.13(9)	149.0
C(51)–H(92)···Cl(2)	1.08	2.56	3.42(9)	136.0
C(58)–H(96)···Cl(2)	1.09	2.61	3.37(11)	126.0

Table 4. The energy and character of selected occupied and virtual MOs for $[RuCl(PPh_3)_2(C_6H_5N_3)(C_5H_4NCO_2)]$.

MO	Energy (eV)	Character
H-15	−6.708	$\pi_{phosphine}$
H-14	−6.682	$\pi_{phosphine}$
H-13	−6.598	π_{Cl}
H-12	−6.584	$\pi_{Cl} + \pi_{phosphine}$
H-11	−6.549	$\pi_{phosphine}$
H-10	−6.495	$\pi_{Cl} + \pi_{phosphine}$
H-9	−6.461	$\pi_{phosphine}$
H-8	−6.434	$\pi_{Cl} + \pi_{phosphine}$
H-7	−6.415	$\pi_{phosphine}$
H-6	−6.303	$\pi_{Cl} + \pi_{phosphine}$
H-5	−6.222	$\pi_{phosphine}$ (n_P)
H-4	−6.147	$\pi_{Cl} + \pi_{phosphine}$
H-3	−6.069	π_O
H-2	−5.352	d_{yz}
H-1	−4.780	$d_{xz} + \pi^*_{Cl}$
Homo	−4.709	$d_{xy} + \pi^*_{Cl} + \pi^*_O$
Lumo	−1.528	$\pi^*_{benzotriazole}$
L + 1	−1.161	$\pi^*_{pyridine\ carboxylate}$
L + 2	−0.667	$\pi^*_{pyridine\ carboxylate}$
L + 3	−0.559	$d_{x^2-y^2} + \pi^*_{phosphine}$
L + 4	−0.402	$\pi^*_{phosphine}$
L + 5	−0.355	$\pi^*_{phosphine}$
L + 6	−0.298	$d_{x^2-y^2} + \pi^*_{phosphine}$
L + 7	−0.128	$\pi^*_{phosphine}$
L + 8	−0.098	$\pi^*_{phosphine} \rightarrow \pi^*_{benzotriazole}$
L + 9	0.011	$\pi^*_{phosphine} \rightarrow \pi^*_{benzotriazole}$
L + 10	0.066	$\pi^*_{phosphine} \rightarrow \pi^*_{benzotriazole}$
L + 11	0.114	$\pi^*_{phosphine} \rightarrow \pi^*_{benzotriazole}$
L + 12	0.220	$\pi^*_{phosphine}$
L + 13	0.250	$d_z^2 + \pi^*_{phosphine}$
L + 14	0.299	$\pi^*_{phosphine}$
L + 15	0.433	$\pi^*_{phosphine}$
L + 16	0.454	$\pi^*_{phosphine}$

In table 4 the energy and character of selected occupied and virtual MOs for $[RuCl(PPh_3)_2(C_6H_5N_3)(C_5H_4NCO_2)]$ are presented. The contours of several HOMO and LUMO molecular orbitals are depicted in figure 3. The d_{yz}, d_{xz}, d_{xy} ruthenium orbitals are HOMO, HOMO-1 and HOMO-2 molecular orbitals with antibonding contributions from π chlorine ligands. The $d_{x^2-y^2}$ and d_z^2 ruthenium orbitals have contributions of the π phosphine LUMO + 6 and LUMO + 13 MOs. The HOMO-3 orbital is localized on the pyridylcarboxylato ligand and the π oxygen orbitals play the

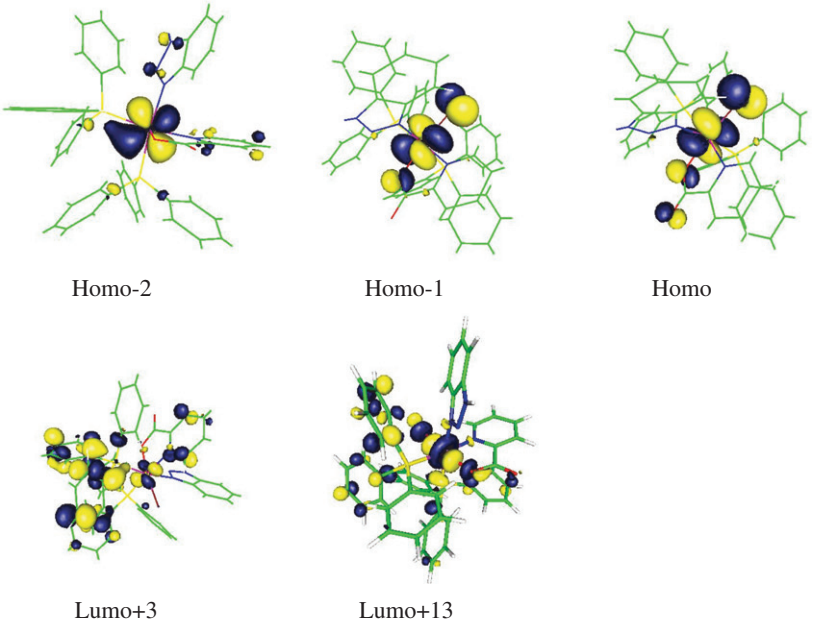

Figure 3. The contours of several HOMO and LUMO molecular orbitals.

Table 5. Calculated electronic transitions for $[RuCl(PPh_3)_2(C_6H_5N_3)(C_5H_4NCO_2)]$ with the TDDFT method.

Most important configurations	Character	E(V)	λ(nm)	f	Exp. λ(nm)(E[eV])log ε
H → L	$d \rightarrow \pi^*_{benzotriazole}$	2.53	490.4	0.0050	
H → L + 1	$d \rightarrow \pi^*_{pyridine\ carboxylate}$	2.77	447.7	0.0034	
H → L + 3	$d \rightarrow d_{x^2-y^2} + \pi^*_{phosphine}$	3.02	410.3	0.0016	381.6(3.25)3.63
H-2 → L	$d \rightarrow \pi^*_{benzotriazole}$	3.10	399.4	0.0213	
H-2 → L + 2	$d \rightarrow \pi^*_{pyridine\ carboxylate}$	3.21	386.3	0.0204	
H-2 → L + 1	$d \rightarrow \pi^*_{pyridine\ carboxylate}$	3.46	358.2	0.0724	
H-2 → L + 2	$d \rightarrow \pi^*_{pyridine\ carboxylate}$	3.98	311.2	0.0211	
H-2 → L + 5	$d \rightarrow \pi^*_{phosphine}$	4.33	286.3	0.0130	
H-2 → L + 8	$d \rightarrow \pi^*_{phosphine/benzotriazole}$	4.60	269.3	0.0118	
H-16 → L	$\pi_{phosphine} \rightarrow \pi^*_{benzotriazole}$	4.72	262.5	0.0207	259.0(4.79)4.33
H-9 → L + 1	$\pi_{phosphine} \rightarrow \pi^*_{pyridine\ carboxylate}$	4.77	259.9	0.0037	
H-3 → L + 3	$\pi_O \rightarrow d_{x^2-y^2} + \pi^*_{phosphine}$	4.88	254.1	0.0237	
H-4 → L + 3	$\pi_{Cl/phosphine} \rightarrow d_{x^2-y^2} + \pi^*_{phosphine}$	4.92	251.8	0.0364	
H-5 → L + 3	$\pi_{phosphine}\ (n_P) \rightarrow d_{x^2-y^2} + \pi^*_{phosphine}$	5.01	247.6	0.0403	
H-6 → L + 3	$\pi_{Cl/phosphine} \rightarrow d_{x^2-y^2} + \pi^*_{phosphine}$	5.11	242.5	0.0276	233.2(5.32)4.64
H-2 → L + 17	$d \rightarrow \pi^*_{phosphine}$	5.13	241.4	0.0153	
					217.2(5.71)4.45

main role. The LUMO results from the benzotriazole nitrogen (49%) and carbon (44%) orbitals.

3.2. *Electronic spectrum*

The investigated complex is large, and the number of basis functions is 938. The hundred electron transitions calculated by the TDDFT method do not comprise all

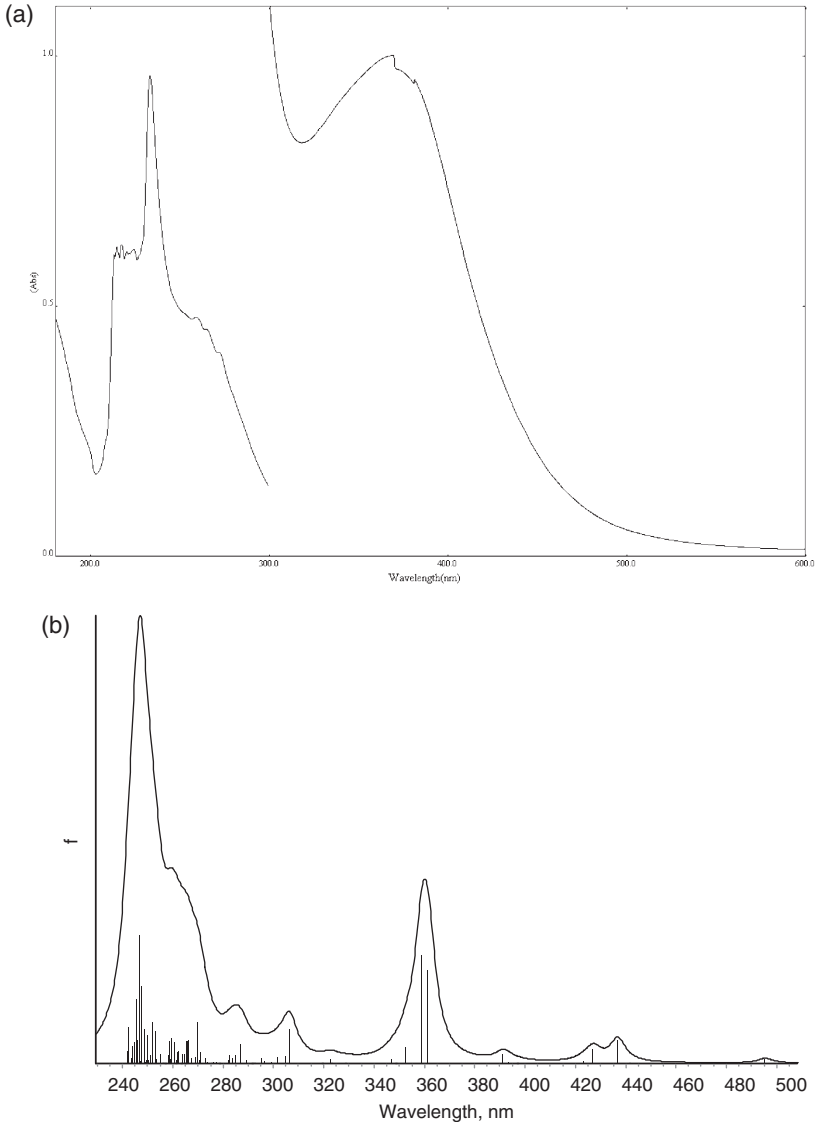

Figure 4. The experimental (a) and calculated (b) electronic spectra of $RuCl(PPh_3)_2(C_6H_5N_3)(C_5H_4NCO_2)$].

the experimental absorption bands. The UV–Vis spectrum was calculated to 240 nm, so the shortest wavelength experimental bands cannot be assigned to calculated transitions. However, considering that the solution spectra of PPh_3, benzotriazole and pyridylcarboxylato ligands exhibit intense absorption bands in 260–200 nm region, some additional intraligand and interligand transitions are expected to be found at higher energies in the calculations.

The calculated electronic transitions are gathered in table 5. The experimental and calculated spectra of $[RuCl(PPh_3)_2(C_6H_5N_3)(C_5H_4NCO_2)]$ are depicted on figure 4(a)

and (b), respectively. The contour of the calculated spectrum was broadened by Lorentzian function calculated by formula:

$$I = \frac{I_0}{1 + (\nu - \nu_0)/\gamma^2}; \quad \text{where } \gamma = 1/2 \text{ of spectral width on } 1/2 \text{ height.}$$

The experimental spectrum of shows a broad, unsymmetrical band between 500 to 330 nm with the maximum at 381.6 nm resulting from Metal Ligand Charge Transfer (MLCT) with contribution of the $d \rightarrow d$ transition. The next experimental band with maximum at 259.0 nm is assigned to transitions calculated between 311.2 nm (3.98 eV) and 251.8 nm (4.92 eV). These transitions are MLCT, LMCT (Ligand Metal Charge Transfer) and Ligand Ligand Charge Transfer (LLCT). The LLCT transitions in this region have interligand character ($\pi_{\text{phosphine}} \rightarrow \pi^*_{\text{benzotriazole}}$, $\pi_{\text{phosphine}} \rightarrow \pi^*_{\text{pyridine carboxylate}}$). The experimental band at 233.2 nm is ascribed to transitions calculated between 247.6 and 241.4 nm. The transition is mainly from phosphine ligand orbitals to $\pi^*_{\text{phosphine}}$ (LLCT character) with admixture of LMCT transition (H-3 → L) and MLCT (H-2 → L + 17).

The experimental band at 217.1 nm (not calculated) is probably also a $\pi_{\text{Ph}} \rightarrow \pi^*_{\text{Ph}}$ transition in the phenyl group of the triphenylphosphine ligand. This transition is calculated in the free triphenylphosphine at about 214 nm (experimental band at 217 nm).

Supplementary material

More details of the crystal structure determinations have been deposited with the Cambridge Crystallographic Data Centre with the deposition number: CCDC 288860.

Acknowledgements

The Gaussian 03 calculations were carried out in the Wrocław Centre for Networking and Supercomputing, WCSS, Wrocław, Poland under calculational grant No. 51/96.

References

[1] M. Yamakawa, H. Ito, R. Noyari. *J. Am. Chem. Soc.*, **122**, 1466 (2000).
[2] S. Chang, L. Jones, C.M. Henling, R.H. Grubbs. *Organometallics*, **17**, 3460 (1998).
[3] B. De Clereq, F. Verpoort. *Macromolecules*, **35**, 8943 (2002).
[4] B. De Clereq, F. Verpoort. *Adv. Synth. Catal.*, **34**, 639 (2002).
[5] T. Opstal, F. Verpoort. *Angew Chem. Int. Ed.*, **42**, 2876 (2003).
[6] B. De Clereq, F. Lefebvre, F. Verpoort. *Appl. Catal. A*, **247**, 345 (2003).
[7] F. Porta, S. Tollari, C. Bianchi, S. Recchia. *Inorg. Chim. Acta*, **249**, 79 (1996).
[8] S.L. Queiroz, A.A. Batista, G. Olivia, M.T.do.P. Gambardella, R.H.A. Santos, K.S. MacFarlane, S.J. Rettig, B.R. James. *Inorg. Chim. Acta*, **267**, 209 (1998).
[9] I.R. Butler, U. Griesbach, P. Zanello, M. Fontani, D. Hibbs, B.M. Hursthouse. *J. Organomet. Chem.*, **565**, 243 (1998).
[10] J.G. Małecki, J.O. Dzięgielewski, R. Kruszynski, T.J. Bartczak. *Inorg. Chem. Commun.*, **6**, 721 (2003).
[11] P.C. Hohenberg, W. Kohn, L.J. Sham. *Adv. Quant. Chem.*, **21**, 7 (1990).
[12] W. Kohn, A.D. Becke, R.G. Parr. *J. Phys. Chem.*, **100**, 12974 (1996).
[13] R.G. Parr, W. Yang. *Ann. Rev. Phys. Chem.*, **46**, 701 (1995).
[14] E.J. Baerends, O.V. Gritsenko. *J. Phys. Chem. A*, **101**, 5383 (1997).

[15] T. Ziegler. *Chem. Rev.*, **91**, 651 (1991).
[16] M.E. Casida. In *Recent Advances in Density Functional Methods*, D.P. Chong (Ed.), Vol. 1, World Scientific, Singapore (1995).
[17] M.E. Casida. In *Recent Developments and Applications of Modern Density Functional Theory, Theoretical and Computational Chemistry*, J.M. Seminario (Ed.), Vol. 4, p. 391, Elsevier, Amsterdam (1996).
[18] M.E. Casida, C. Jamorski, K.C. Casida, D.R. Salahub. *J. Chem. Phys.*, **108**, 4439 (1998).
[19] C. Adamo, V. Barone. *Theor. Chem. Acta*, **105**, 169 (2000).
[20] S.J.A. van Gisbergen, J.A. Groeneveld, A. Rosa, J.G. Snijders, E.J. Baerends. *J. Phys. Chem. A*, **103**, 6835 (1999).
[21] A. Rosa, E.J. Baerends, S.J.A. van Gisbergen, E. van Lenthe, J.A. Groeneveld, J.G. Snijders. *J. Am. Chem. Soc.*, **121**, 10356 (1999).
[22] A. Dreuw, M. Head-Gordon. *J. Am. Chem. Soc.*, **126**, 4007 (2004); A. Dreuw, J.L. Weisman, M. Head-Gordon. *J. Chem. Phys.*, **119**, 2943 (2003); O. Gritsenko, E.J. Baerends. *J. Chem. Phys.*, **121**, 655 (2004).
[23] S. Záliš, N. Ben Amor, C. Daniel. *Inor. Chem.*, **43**, 7978 (2004).
[24] V.Yu. Kukushkin, A.J.L. Pombeiro. *Inorg. Chim. Acta*, **358**, 1 (2005).
[25] T.A. Stephenson, G. Wilkonson. *J. Inorg. Nucl. Chem.*, **28**, 945 (1966).
[26] X-RED. Version 1.18. STOE & Cie GmbH, Darmstadt, Germany (1999).
[27] G.M. Sheldrick. *Acta Cryst.*, **A46**, 467 (1990).
[28] G.M. Sheldrick. *SHELXL-97 Program for the Solution and Refinement of Crystal Structures*, University of Göttingen, Germany (1997).
[29] G.M. Sheldrick. *SHELXTL: Release 4.1 for Siemens Crystallographic Research Systems*, Madison, WA (1990).
[30] M.J. Frisch, G.W. Trucks, H.B. Schlegel, G.E. Scuseria, M.A. Robb, J.R. Cheeseman, J.A. Montgomery Jr, T. Vreven, K.N. Kudin, J.C. Burant, J.M. Millam, S.S. Iyengar, J. Tomasi, V. Barone, B. Mennucci, M. Cossi, G. Scalmani, N. Rega, G.A. Petersson, H. Nakatsuji, M. Hada, M. Ehara, K. Toyota, R. Fukuda, J. Hasegawa, M. Ishida, T. Nakajima, Y. Honda, O. Kitao, H. Nakai, M. Klene, X. Li, J.E. Knox, H.P. Hratchian, J.B. Cross, C. Adamo, J. Jaramillo, R. Gomperts, R.E. Stratmann, O. Yazyev, A.J. Austin, R. Cammi, C. Pomelli, J.W. Ochterski, P.Y. Ayala, K. Morokuma, G.A. Voth, P. Salvador, J.J. Dannenberg, V.G. Zakrzewski, S. Dapprich, A.D. Daniels, M.C. Strain, O. Farkas, D.K. Malick, A.D. Rabuck, K. Raghavachari, J.B. Foresman, J.V. Ortiz, Q. Cui, A.G. Baboul, S. Clifford, J. Cioslowski, B.B. Stefanov, G. Liu, A. Liashenko, P. Piskorz, I. Komaromi, R.L. Martin, D.J. Fox, T. Keith, M.A. Al-Laham, C.Y. Peng, A. Nanayakkara, M. Challacombe, P.M.W. Gill, B. Johnson, W. Chen, M.W. Wong, C. Gonzalez, J.A. Pople. *Gaussian 03, Revision B.03*, Gaussian, Inc., Pittsburgh, PA (2003).
[31] B. Mennucci, J. Tomasi. *J. Chem. Phys.*, **106**, 5151 (1997).
[32] A.D. Becke. *J. Chem. Phys.*, **98**, 5648 (1993).
[33] C. Lee, W. Yang, R.G. Parr. *Phys. Rev. B*, **37**, 785 (1988).
[34] N. Godbout, D.R. Salahub, J. Andzelm, E. Wimmer. *Can. J. Chem.*, **70**, 560 (1992).
[35] R. Mukherjee. *Coord. Chem. Rev.*, **203**, 151 (2000).
[36] I.D. Brown. *Acta Cryst.*, **B53,**, 381 (1997).
[37] T. Hirano, M. Kuroda, N. Takeda, M. Hayashi, M. Mukaida, T. Oi, H. Nagao. *J. Chem. Soc., Dalton Trans.*, 2158 (2002).
[38] L. Sieron, M. Bukowska-Strzyzewska. *Acta Cryst.*, **C55**, 1230 (1999).
[39] G.R. Desiraju, T. Steiner. *The Weak Hydrogen Bond in Structural Chemistry and Biology*, Oxford University Press (1999).
[40] G.A. Jeffrey, W. Saenger. *Hydrogen Bonding in Biological Structures*, Springer-Verlag (1994).